



Structural Variations in SBA-15 by Copper Incorporation and a Test in Catalytic Wet Peroxide Oxidation of Phenol

Filiz AKTI^{1,*} , Suna BALCI¹ ¹ Gazi University, Faculty of Engineering, Chemical Engineering Department, 06570, Ankara, Turkey

Article Info

Received: 06/08/2018

Accepted: 06/11/2018

Keywords

Cu-SBA-15
Catalytic wet peroxide
oxidation
Phenol

Abstract

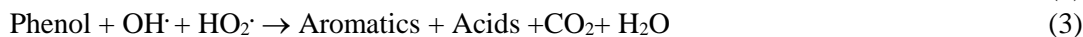
This study presents the phenol removal in the wastewater via catalytic wet peroxide oxidation over Cu-SBA-15 catalyst. The hydrothermally synthesized copper catalyst was characterized using XRD, N₂ adsorption-desorption isotherms and FTIR analysis techniques. The multiple BET surface area, total pore volume and mesopore diameter values were determined as 996 m²/g, 1.55 cm³/g and 6.82 nm, respectively. XRD pattern showed that the copper loading did not demolish the characteristic structure of SBA-15. FTIR spectrum of SBA-15 and catalyst without and with pyridine sorption showed the enhancement both in Lewis and Brønsted acidities by copper incorporation to the structure. The wet hydrogen peroxide catalytic oxidation of phenol performed in a batch reactor at 25, 40 and 60 °C temperatures provided 56% phenol conversion at 60 °C.

1. INTRODUCTION

Phenol compounds found in waste of several industries such as petrochemical oil refinery, iron– steel mills and dye producing are toxic even at low concentrations. Phenol removal is still an important due to serious problem on human health [1, 2]. Some techniques such as physical (adsorption, solvent extraction, filtration, ion exchange and precipitation), biological and chemical (advanced oxidation and ozonation) are used for the phenol removal from wastewater [3-6]. In the case of high concentration application by physical method, the desired level of phenol concentration is not achieved. Although biodegradation is generally applied to reach the desired as ultra–separation, it is insufficient for resistive phenol. In recent years, advanced oxidation processes (AOP) techniques come in front among various chemical process technologies. AOP techniques usually performed the degradation of phenol with suitable oxidants such as oxygen (air), ozone and hydrogen peroxide over a solid catalyst. AOP based on the production of many hydroxyl radicals quickly oxidize many organic contaminants to less harmful intermediates with these radicals. It is also stated that when appropriate oxidation conditions are provided, complete mineralization to final products such as carbon dioxide and water can be reached by advanced oxidation processes [7, 8]. Catalytic wet air oxidation (CWAO) is generally requires high pressure and temperature. Catalytic wet peroxide oxidation (CWPO) is an effective and clean treatment as compared with other catalytic oxidation processes and it can be operated under mild condition close to atmospheric values with low energy consumption [9-13]. When homogeneous catalysts used in CWPO reactions, the catalyst is not preferred as long as the recovery and sufficient pH range are limited and use of heterogeneous catalysts overcomes these drawbacks [14]. In the CWPO processes, transition metals such as copper, iron, chromium, manganese, ceria and cobalt are preferred generally for the formation of hydroxyl radicals which are formed by the redox processes between transition metal and hydrogen peroxide [1, 15-17]. In recent years, copper catalysts based support such as mesoporous silica, alumina, active carbon, zeolite and clays have been preferred in CWPO of phenol due to their excellent properties such as suitable in large pH working range, good redox features and high catalytic activities [18-20].

*Corresponding author, e-mail: filizakti@gazi.edu.tr

In the heterogeneous CWPO of phenol carried out using copper catalyst, copper species reacts with hydrogen peroxide, leading to the formation of hydroxyl, which direct to the degradation of phenol molecules.



where S^* is reachable redox surface sites of the copper species [21, 22]. In the first step, the $OH\cdot$ radicals are formed by the reaction of H_2O_2 molecule with the CuO active site and then the generation of aromatic compounds (catechol, hydroquinone and resorcinol) is occurred. Aromatic rings are attacked by generated $OH\cdot$ radicals which lead to partial oxidation. These organic compounds are broken down to form some by products such as oxalic acid, maleic acid, acetic acid, malonic acid and formic acid. At last, these organic acids lead to CO_2 and H_2O formation [18].

Physicochemical properties of the support such as surface functional groups, pore size distribution and surface area are important in catalytic activity [23]. The highly ordered hexagonally channeled SBA-15 (Santa Barbara Amorphous-15) having many advantages such as narrow and uniform pore size distribution, large pore size (4.6-30 nm) and pore volume, high surface area (800-1000 m^2/g), thick pore wall (3-9 nm), hydrothermal stability and these properties make the SBA-15 as a good support alternative. Otherwise finding high amount of silanol groups (Si-OH) on its surface provides binding of organic molecules [23-26]. As it is known, in the impregnation method the success of incorporation of metal compounds on the catalyst surface is high, but there are disadvantages such as two-stage production with more energy usage, distribution of non-homogeneous active component, blocking of pores and reduction of surface area. Moreover, metal loss higher than that of hydrothermal method in the filtration step. The hydrothermal method provides economical superiority because it is a one-stage production and it provides the homogeneous distribution of the active ingredient to each other while also protecting the pore structure of the support [27, 28]. Literature studies indicated the metal dissolution problems in the use of metal impregnated catalysts. [29-31].

The studies performed with copper SBA-15 catalysts have been limited for CWPO of phenol [18, 32]. Liou et al. [14] observed phenol conversion over 90% by use of copper activated carbon catalysts at 80 °C in CWPO. Garrido et al. [33] obtained phenol conversion 100% using copper-alumina-silica-clay catalysts in the CWPO of phenol for 300 min at 40°C. Wang et al. [34] synthesized hydrothermally synthesized catalysts with copper active metal over supports such as SBA-15 and HMS. Phenol conversion over Cu-SBA-15 and CuHMS catalysts determined as 59.4 and 32.7, respectively. As seen in these studies, catalysts obtained by impregnation method showed higher phenol removal.

In the present study, Cu-SBA-15 material was synthesized hydrothermally and was tested in the CWPO of phenol. The characterization of materials was performed by XRD (X-Ray diffraction), N_2 adsorption-desorption and FTIR (Fourier transform infrared) techniques and the effects of physical and chemical properties of samples on the phenol conversion were investigated.

2. EXPERIMENTAL

Pluronic 123 (PEO20PPO70PEO20, Sigma-Aldrich) and TEOS (tetraethyl ortosilicate, Merck) were used as template and silica source, respectively. Hydrochloric acid (Merck) was used as acid source and water as solvent. Copper nitrate ($Cu(NO_3)_2 \cdot 3H_2O$, Merck) was selected as copper source. Phenol (Merck) and hydrogen peroxide (H_2O_2 , Merck) was selected as a model organic pollutant and oxidant for wet oxidation test, respectively. All reagents were of analytical grade.

The synthesis of SBA-15 support was performed according to studies of Zhao et al. [24]. In the synthesis of Cu-SBA-15 catalyst, copper source was added to the synthesis solution before TEOS addition and Cu/Si molar ratio was taken as 0.03. Synthesis was carried out in autoclave at 100 °C for 2 days, obtained gel was filtered firstly, washed with deionized water and then obtained solid was allowed dry at room temperature.

Finally calcination of dried solid powders was done at 550 °C for 6 h after heating with a heating rate of 1 °C/min.

XRD patterns were collected within $0.5 < 2\theta < 90^\circ$ range with step size of 0.02° and step time of 0.025 s from a Philips PW 3040 diffractometer equipment using $\text{CuK}\alpha$ -radiation ($\lambda=0.15406$ nm). N_2 adsorption-desorption isotherm of samples dried for 24 h at 110 °C and 10^{-7} outgassed at 300 °C under high vacuum (10^{-7} bar) for 3h were obtained using a Quantochrome Autosorb 1C instrument within the relative pressure (P/P_0) values of 10^{-6} - 0.99. Multiple point BET surface and external surface area values were calculated from isotherm data between $0.05 < P/P_0 < 0.30$ and the t-plot method using de-Bore thickness, respectively. Total pore (V_{total}) and micro+meso pore ($V_{\text{micro+meso}}$) volumes were determined from the amount of N_2 adsorbed at $P/P_0=0.99$ and 0.96, respectively. The t-plot was again applied for calculating the micropore volume (V_{micro}). The mesopore volume (V_{meso}) was calculated from the difference between micro+mesopore volume and micropore volume ($V_{\text{micro+meso}} - V_{\text{micro}}$). Barrett-Joyner-Halenda method (BJH-method) and Saito-Foley method (SF-method) were applied to the adsorption data at $0.35 < P/P_0 < 0.99$ for mesopore and $10^{-7} < P/P_0 < 0.30$ for micropore regions, respectively for determination of pore size distribution [35]. FTIR spectrums were recorded on a Bruker Vertex 70/70v FTIR spectrometer. Before analyses, samples were dried at 100 °C in oven and then 1 g sample was diluted with 100 g KBr after then samples were transferred DRIFT cell of FTIR. Samples were exposed to pyridine probe molecules at room temperature in the vacuum desiccators (vacuum around 10^{-6} bar) to determine acid site. In order to determine the settling of phenol which sites/region on the copper catalyst, phenol was dropped over catalyst and then dried at room temperature and analyzed with FTIR.

The CWPO of phenol was studied using a 250 mL volume of batch reactor at 25, 40 and 60 °C and atmospheric pressure under mixing. 0.02 g Cu-SBA-15 sample was introduced into 20 mL of 50 ppm phenol solution under continuous stirring. 0.1 mol/L H_2O_2 solution was added continuously (total of 9 mL) to the phenol-catalyst mixture with a flow rate of 0.1 mL/min. 1 mL aliquots were taken from the reactor in regular time intervals and it was filtered using a 0.22 μm nylon filter. The phenol concentrations were measured with a Perkin-Elmer Lambda 35 UV-VIS spectrophotometer at a 270 nm wavelength.

3. RESULTS AND DISCUSSION

3.1. Characterization of Samples

The XRD patterns and d_{100} , unit cell parameter (a) and pore wall thickness (δ) of samples are given in Fig. 1 and Table 1, respectively. The typical peaks of SBA-15 were obtained at 2θ : 0.83° (100), 1.46° (110), 1.67° (200) and amorphous silica wall at 2θ : $18-35^\circ$ which this values was compatible with the results of Zhao et al. [24]. The narrow and high peak intensity (100) reflections of samples indicated a good mesopore ordering and the typical hexagonal channels of SBA-15. Copper incorporation to the SBA-15 structure did not change the position of 100 and 200 reflections. (100) plane reflections preserved narrow peak which is supported did not destroy of the mesopore ordering. Significant increase in the (100) plane diffraction showed the formation of long channels (Fig 1a) [36]. Although 100-spacing ($d_{100} = 10.6$ nm) and lattice parameter (12.3 nm) values remained the same, the pore wall thickness value decreased a little (0.09 nm).

In the wide angle XRD patterns of Cu-SBA-15 (Fig 1b) no reflections typical of copper species could be observed, only observed broad peak (at $20-30^\circ$ Bragg angle) indicative of the amorphous silica structure [24]. This could be caused by settling of metal compounds into silica wall or formation of small crystallite form of metal complexes with the size of below XRD detection limit (~ 3 nm) [37].

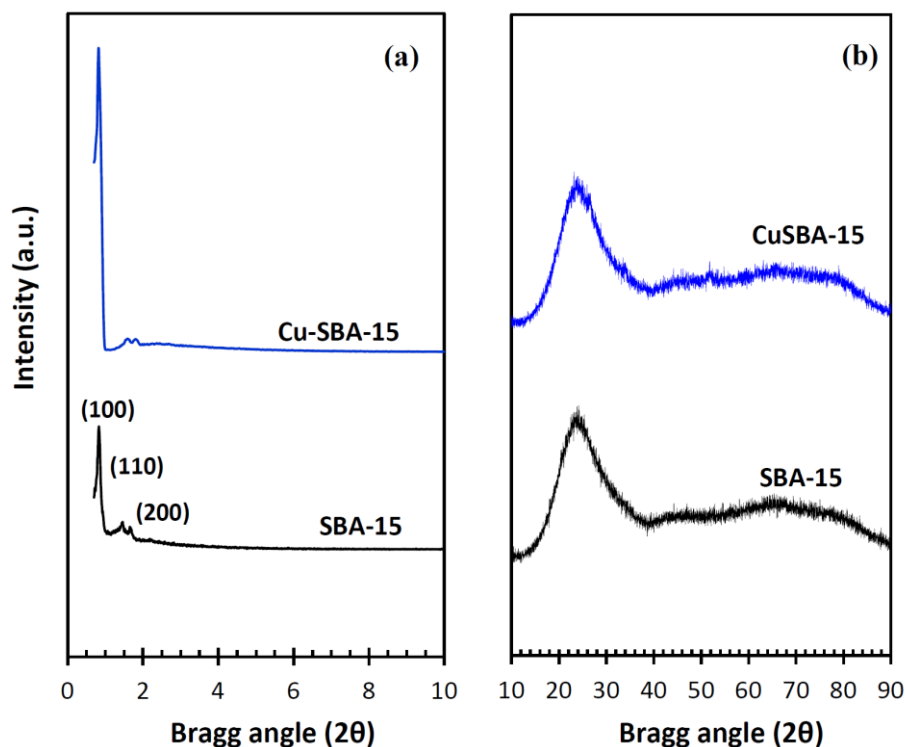


Figure 1. XRD patterns of SBA-15 and Cu-SBA-15 (a) small angle region (b) wide angle region

The N_2 adsorption-desorption isotherms of samples given in the Fig. 2. All samples exhibited a well-defined opening hysteresis loop in the $P/P_0=0.60-0.78$. It corresponds to the type IV with H1 hysteresis loops of IUPAC classification and is a representative of mesoporous texture with well-ordered cylindrical pores. The significant increases of adsorbed gas volumes for relative pressure values below 0.3 and consequently at 0.99 were resulted from textural ameliorations by copper addition [4, 35, 38]. The hysteresis loop of Cu-SBA-15 was started at a value higher P/P_0 than that of SBA-15. This behavior was related to the formation of little higher mesopore diameter and sharpness in this step indicated the uniformity of the mesopores with a good mesoporous structural ordering and relatively narrow pore size distribution [39]. This hysteresis behavior corresponding to capillary condensation of nitrogen, also consistent with the XRD results as an indicator of the uniformity of the pores (Fig. 2). As seen from isotherms, adsorbed gas volume of Cu-SBA-15 material has been 1.5 times higher than that of SBA-15 in the mesopore and micropore regions. The high rise in nitrogen uptake within the mesopore region was the indicative of higher pore volumes and surface areas than those of SBA-15. All surface area values were increased with copper incorporation by the increases in the pore volume values. The pore size distribution curves are given in Fig.3 and results are summarized in Table 1. The pore size distributions of materials exhibited a wide distribution at micropore region while a narrow, sharp and homogenous distribution at was seen in mesopore region. These narrow and sharp peaks in mesopore size distribution curves were again the demonstration of mesopore homogeneity. The average pore diameter of SBA-15 was obtained as 0.92 nm by using SF-method at micropore region and also as 6.73 nm by using BJH-method at mesopore region. While the mesopore pore diameter of Cu-SBA-15 increased, micropore diameter decreased a little showing the formation of more microporous silica walls. Especially improvement in pore size distribution in the micropore region reflected to surface area value. The formation of new small pores within the thickening silica pore walls and metal-silica phases by copper insertion generally reflected small increases in the adsorbed pore volumes in the micropore range of the isotherm and average micropore sizes shifted to a little higher value.

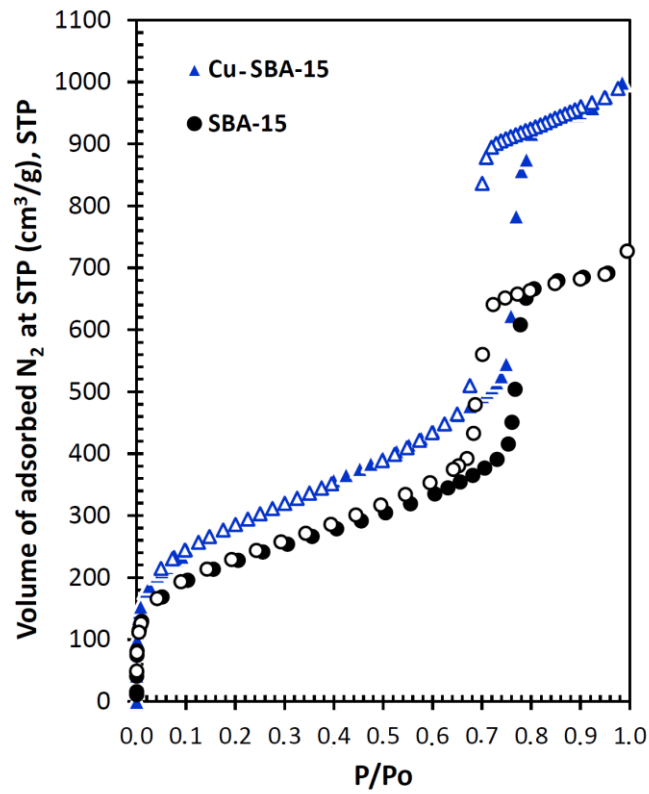


Figure 2. N₂ adsorption-desorption isotherms of SBA-15 and Cu-SBA-15

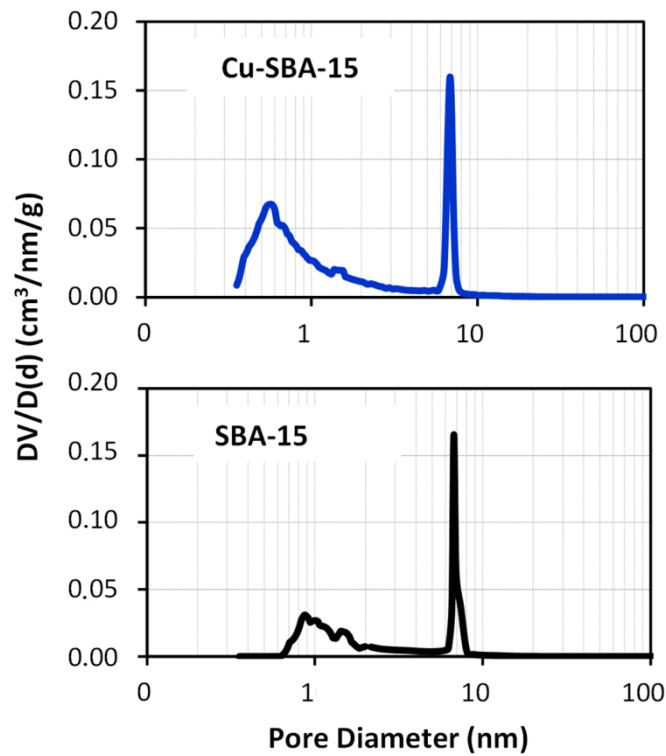


Figure 3. Pore size distribution of SBA-15 and Cu-SBA-15

Table 1. Physically properties of SBA-15 and Cu-SBA-15

Material	XRD lattice parameter (nm)			Pore volume (cm ³ /g)			Pore diameter (nm)		Surface area (m ² /g)	
	d ₁₀₀	a	δ	V _{micro}	V _{meso}	V _{total}	BJH method	SF method	Multiple BET	External surface area
SBA-15	10.6	12.3	5.57	0.58	0.64	1.14	6.73	0.92	800	118
Cu-SBA-15	10.6	12.3	5.48	0.73	0.79	1.55	6.82	0.56	996	190

d₁₀₀: basal spacing; a: lattice parameter ($= 2 \times d_{(100)}/\sqrt{3}$); δ: wall thickness ($= a - \text{pore diameter}$)

FTIR spectrums for samples are given in Fig.4. FTIR spectrums in the 400–2000 cm⁻¹ of all samples showed that bending vibrations resulting from typical silica material. The bands observed at 1080 cm⁻¹, 804 cm⁻¹ and 484 cm⁻¹ corresponding to bend stretching vibration bands of Si–O–Si, symmetric and asymmetric, respectively. The band appeared at about 960 cm⁻¹ was resulted from Si–OH stretching band. Loading of copper to SBA-15 structure didn't significantly affect the main peaks in this silica region [34, 40-43]. The intensity of this peak didn't change with copper incorporation.

The broad band observed within 3000–3700 cm⁻¹ range is assigned to associated peak of hydroxyl groups. This broad band was significantly decreased with copper loading [44-46]. The sharp peak at 3745 cm⁻¹ is known to be caused by vibrations of the Si–OH [41, 47]. The intensity of this band was increased due to the bonding of copper to the free silanol groups with the copper incorporation. The evident aliphatic stretching C–H at ~1407 cm⁻¹ and C–O at ~1874 cm⁻¹ bands which are more prominent in Cu-SBA-15 catalyst could be resulted from the left organic template in the structure.

The band which appears at 1446 cm⁻¹ is ascribed to physisorbed pyridine. The observed band at 1629 cm⁻¹ can be distinguishing coordinately bonded pyridine; however, the O–H bending frequency of adsorbed water occurs in the same region and may interfere [48]. The intensity of this peak decreased after pyridine sorption due to pyridine adsorption carried out under high vacuum caused the removal of adsorbed water and a new peak were obtained at 1598 cm⁻¹ which assigned to hydrogen bonded pyridine [49, 50].

The peak at 1490 cm⁻¹ due to the contribution of Brønsted +Lewis acid sites and the ones at 1544 and 1633 cm⁻¹ belonging to Brønsted acid sites were seen in the all samples. The peak at 1579 cm⁻¹ was related to weak Lewis bound pyridine. Pyridine chemisorbed as the pyridinium ion can be distinguished by the band at 1641 cm⁻¹ [46, 51]. The observed 1500, 1512 and 1527 cm⁻¹ bands due to protonated pyridine [52]. Generally, copper incorporation to the SBA-15 structure caused to improvement and the formation of new acid sites.

The model pollutant phenol used in the catalytic activity tests was adsorbed the Cu-SBA-15 to comment on successive bonding of phenol molecule to functional groups over catalyst (Figure 4). An increase in intensity of peak at 1630 cm⁻¹ due to –OH molecule of phenol was occurred. Peak at nearby 3745 cm⁻¹ was seen that the –OH groups and this peak has shown an increase in phenol adsorbed Cu-SBA-15. It seen that phenol molecule was adsorbed mostly on the basic regions (Si–OH and –OH sites) [23, 53].

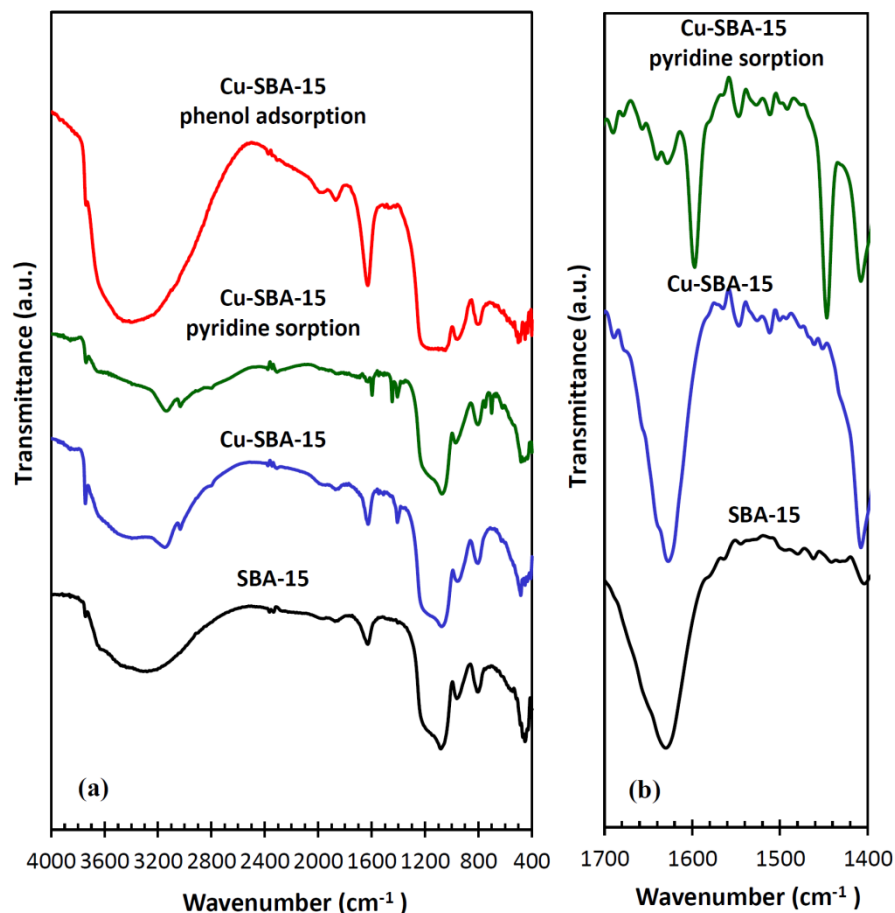


Figure 4. FTIR spectrums of samples in the region of (a) 400-4000 cm^{-1} (b) 1400-1700 cm^{-1}

3.2. Catalytic Activity Test

The catalytic activity results of the copper catalyst are shown in Fig. 5. The phenol conversion was found as 21 % at 25 °C and reached to 56 % within 60 minutes by the increasing of temperature to 60 °C. In the study of Valkaj et al. [30] carried by the hydrothermally synthesized Cu/ZSM5 ~ 66% phenol removal was achieved in a 180 minute at the same temperature and Wang et al. [34] obtained 59.4 % and 32.7% phenol conversion by use of hydrothermally synthesized copper catalysts with SBA-15 and HMS support for CWPO. The surface area (728 m^2/g) and pore volume (0.81 cm^3/g) values of Cu-SBA-15 catalysts lower than that of our catalyst that this behavior is an advantage. Molecular size of hydrogen peroxide and phenol is 0.2476 and 0.4297 nm, respectively [21]. Therefore, they would diffuse more easily in the pores of Cu-SBA-15 as 6.82 nm. On the other hand, there is a significant increase at the oxidation rate due to the increase of temperature resulting increases in kinetic energy of molecules. Redox properties of copper cations assisted the formation of active hydroxyl radicals in the presence of hydrogen peroxide and acidity of catalyst influenced the hydrogen peroxide conversion which provided the highest hydroxyl radicals generation rate [21]. Brønsted acidity play important role in the CWPO of phenol and the presence of structural OH species which promoted Brønsted acidity had been related with catalytic efficiency. From this point of view, the synthesized catalyst has been found to provide these properties.

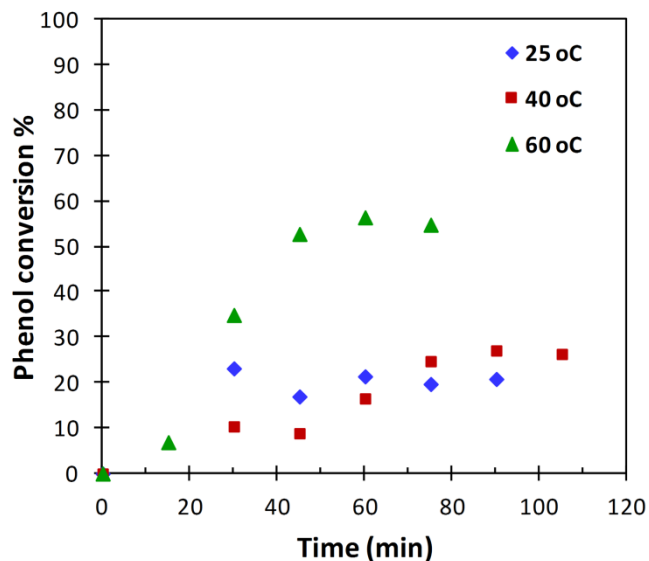


Figure 5. Catalytic activity of the Cu-SBA-15 (at temperature of 25, 40 and 60 °C, atmospheric pressure, 60 ppm initial phenol concentration)

3.2. Conclusions

The surface area, pore diameter, pore volume, surface functional groups and acidity of catalyst effects activity in catalytic oxidation reactions. In this sense, Cu-SBA-15 was successfully synthesized for CWPO of phenol. Phenol molecule was diffused easily into pore due to the pore diameter values of material is bigger than molecule diameter of phenol. Cu-SBA-15 provided necessary acid sites which are Lewis and Brønsted. Phenol molecule was adsorbed especially on finding regions of Si–OH and –OH groups. The increase temperature caused to the increasing of phenol conversion. Cu-SBA-15 material provided the phenol conversion of 56% at 60 °C.

CONFLICTS OF INTEREST

No conflict of interest was declared by the authors.

REFERENCES

- [1] Catrinescu, C., Teodosiu, C., Macoveanu, M., Miche-Brendle, J., Dred, R., “Catalytic wet peroxide oxidation of phenol over Fe- exchanged pillared beidellite”, *Water Res.*, 37: 1154–1160, (2003).
- [2] Taran, O.P., Zagoruiko, A.N., Yashnik, S. A., Ayusheev, A. B., Andrey V., Prosvirin, I.P., Prihod'kof, R.V., Goncharukf, V.V., Parmon, V.N., “Wet peroxide oxidation of phenol over carbon/zeolite catalysts. Kinetics and diffusion study in batch and flow reactors”, *J. Environ. Chem. Eng.*, 6: 2551–2560, (2018).
- [3] Damjanovic, L., Rakic, V., Rac, V., Stosic, D., Auruox, A., “The investigation of phenol removal from aqueous solutions by zeolites as solid adsorbents”, *J.Hazard. Mat.*, 184: 477– 484, (2010).
- [4] Garrido-Ramirez, E. G., Theng, B. K. G. Mora, M. L., “Clays and oxide minerals as catalysts and nanocatalysts in Fenton-like reactions—a review”, *App. Clay Sci.*, 47 (3–4): 182–192, (2010).
- [5] Moyo, M., Mutare, E., Chigondo F., Nyamunda, B.C., “Removal of phenol from aqueous by adsorption on yeast, *Saccharomyces Cerevisiae*”, *IJRRAS*, 11: 3, (2012).

- [6] Zhong, M., Wang, Y., Yu, J., Tian, Y., Xu, G., "Porous carbon from vinegar lees for phenol adsorption", *Particuology*, 10: 35–41, (2012).
- [7] Alejandro A., Medina F., Salagre P., Fabregat A., Sueiras J.E. "Characterization and activity of copper and nickel catalysts for the oxidation of phenol aqueous solutions." *Applied Catalysis B: Environmental*, 18: 307–315, (1998).
- [8] Rokhina E.V. Virkutyte J. "Environmental application of catalytic processes: Heterogeneous liquid phase oxidation of phenol with hydrogen peroxide." *Critical Reviews in Environmental Science and Technology*, 41: 125-167, (2011).
- [9] Kim, K.H., Ihm, S.K., "Heterogeneous catalytic wet air oxidation of refractory organic pollutants in industrial wastewaters: A review", *Journal of Hazardous Materials*, 186: 16–34, (2011).
- [10] Kulkarni S.J, Kaware J.P., "Review on research for removal of phenol from wastewater", *Int. J. Sci. Res. Publ.*, 3: 1–4, (2013).
- [11] Divate, S.B., Hinge, R.V., "Review on research removal of phenol from wastewater by using different methods", *International Journal of Scientific and Research Publications*, 5: 1-3, (2014).
- [12] Cordova Villegas, L.G., Mashhadi, N., Chen, M., Mukherjee, D., Taylor, K.E., Biswas, N.A., "Short Review of Techniques for Phenol Removal from Wastewater", *Curr Pollution Rep.*, 2: 157–167, (2016).
- [13] Emgili, H., Yabalak, Erdal., Görmez, Ö., Gizir, A.M., "Degradation of Maxilon Blue GRL Dye using subcritical water and ultrasonic assisted oxidation methods", *G.U. J. Sci.*, 30(4): 140-150, (2017).
- [14] Liou, R.M., Chen, S.H., "CuO impregnated activated carbon for catalytic wet peroxide oxidation of phenol", *J. Hazard. Mater.*, 172: 498–506, (2009).
- [15] Villota, N., Mijangos, F., Varona, F., Andr'es, J., "Kinetic modelling of toxic compounds generated during phenol elimination in wastewaters", *Int. J. Chem. React. Eng.*, 5: A63 (2007).
- [16] Hosseini, S.A., Davodian, M., Abbasian, A.R., "Remediation of phenol and phenolic derivatives by catalytic wet peroxide oxidation over Co-Ni layered double nano hydroxides", *J. Taiwan Inst. Chem. Eng.*, 75: 97–104, (2017).
- [17] Singh, L., Rekha, P., Chand, S., "Comparative evaluation of synthesis routes of Cu/zeolite Y catalysts for catalytic wet peroxide oxidation of quinoline in fixed-bed reactor", *Journal of Environmental Management*, 215: 1–12, (2018).
- [18] Zhong, Xin, Barbier Jr., J., Duprez, Daniel, Zhang, H., Royer, S., "Modulating the copper oxide morphology and accessibility by using micro-/mesoporous SBA-15 structures as host support: Effect on the activity for the CWPO of phenol reaction", *App. Catal. B: Environ.*, 121–122: 123–134, (2012).
- [19] Jiang, S., Zhang, H., Yan, Y., "Cu-MFI zeolite supported on paper-like sintered stainless fiber for catalytic wet peroxide oxidation of phenol in a batch reactor", *Separation and Purification Tech.*, 190: 243–251, (2018).
- [20] Songshan, J., Huiping, Z., Ying, Y., "Cu-MFI zeolite supported on paper-like sintered stainless fiber for catalytic wet peroxide oxidation of phenol in a batch reactor", *Separation and Purification Tech.*, 190: 243–251, (2018).

- [21] Valkaj, K.M., Wittine, O., Margeta, K., Granato, T., Katovi a, A., Zrn evia, S., "Phenol oxidation with hydrogen peroxide using Cu/ZSM5 and Cu/Y5 catalysts", *Polish J. Chem. Tech.*, 13 (3): 28–36, (2011).
- [22] Dom nguez, C.M., Quintanilla, A., Casas, J.A., Rodriguez, J.J., "Kinetics of wet peroxide oxidation of phenol with a gold/activated carbon catalyst", *Chem.Eng.J.*, 253: 486–492, (2014).
- [23] Busca, G., Berardinelli, S., Resini, C., Arrighi, L., "Technologies for the removal of phenol from fluid streams: A short review of recent developments", *J.Hazard. Mat.*, 160: 265–288, (2008).
- [24] Zhao, D., Huo, Q., Feng, J., Chmelka, B.F., Stucky, G.D., "Nonionic triblock and star diblock copolymer and oligomeric surfactant syntheses of highly ordered, hydrothermally stable, mesoporous silica structure", *J. Am.Chem.Soc.*, 120: 6024–6036, (1998).
- [25] Zhao, D., Feng, J., Huo, Q., Melosh, N., Fredrickson, G.H., Chmelka, B.F., Stucky, G.D., "Triblock Copolymer Syntheses of Mesoporous Silica with Periodic 50 to 300 Angstrom Pores", *Science*, 279:548-552 (1998).
- [26] Sanabria, N. R., Molina R., Moreno, S., "Development of pillared clays for wet hydrogen peroxide oxidation of phenol and its application in the post treatment of coffee wastewater", *International Journal of Photoenergy*, Volume 2012, Article ID 864104, 17 pages.
- [27] Augustine, R.L., "Heterogeneous catalysis for the synthetic chemist", Marcel Dekker, New York, (1996).
- [28] Carlo P., Pierluigi V., "Catalyst preparation methods", *Catalysis Today*, 34:281-305, (1997).
- [29] Barrault, J., Bouchoule, C., Echachoui, K., Frini-Srasra, N., Trabelsi, M., Bergaya, F., "Catalytic wet peroxide oxidation (CWPO) of mixed (Al-Cu)-pillared clays", *Appl. Catal B: Environ.*, 15: 269-274, (1998).
- [30] Valkaj, K. M., Katovic, A., Zrn evi , S., "Investigation of the catalytic wet peroxide oxidation of phenol over different types of Cu/ZSM-5 catalyst", *J. Hazard. Mater.* 144 (3): 663–667, (2007).
- [31] Tomul, F., "The effect of ultrasonic treatment on iron–chromium pillared bentonite synthesis and catalytic wet peroxide oxidation of phenol", *Applied Clay Science*, 120: 121–134 (2016).
- [32] Melero, J.A., Calleja, G., Mart nez, F., Molina, R., "Nanocomposite of crystalline Fe₂O₃ and CuO particles and mesostructured SBA-15 silica as an active catalyst for wet peroxide oxidation processes", *Catal. Commun.*, 7: 478–483, (2006).
- [33] Garrido-Ramirez, E.G., Sivaiah, M.V., Barrault, Jo el, Valange, Sabine, Theng, B.K.G., Ureta-Za artu, M. S., Mora, M. L., "Catalytic wet peroxide oxidation of phenol over iron or copper oxide-supported allophane clay materials: Influence of catalyst SiO₂/Al₂O₃ ratio", *Microporous and Mesoporous Mat.* 162: 189–198, (2012).
- [34] Wang, L., Kong A., Chen, B., Ding, H., Shan, Y., He. M., "Direct synthesis, characterization of Cu-SBA-15 and its high catalytic activity in hydroxylation of phenol by H₂O₂. *J. Mol. Catal. A: Chem.*, 230: 143–150, (2005).
- [35] Lowell S, Shields JE, Thomas MA, Thommes M.M., "Characterization of porous solids and powders: surface area and pore size and density", Kluwer Academic Publishers, New York, (2006).

- [36] Ungureanu, A., Dragoi B., Hulea, V., Cacciaguerra, T., Meloni, D., Solinas, V., Dumitriu, E., “Effect of aluminium incorporation by the “pH-adjusting” method on the structural, acidic and catalytic properties of mesoporous SBA-15”, *Microporous and Mesoporous Mat.*, 163: 51–64, (2012).
- [37] Chirieac, A., Dragoi, B., Ungureanu, A., Ciotonea, C., Mazilu, I., Royer, S., Mamede, A.S., Rombi, E., Ferino, I., Dumitriu, E., “Facile synthesis of highly dispersed and thermally stable copper-based nanoparticles supported on SBA-15 occluded with P123 surfactant for catalytic applications”, *J. Catal.*, 339: 270–283, (2016).
- [38] Øye, G., Sjöblom, J., Stöcker, M., “Synthesis, characterization and potential applications of new materials in the mesoporous range”, *Adv. Colloid and Interface Sci.*, 89-90: 439-466, (2001).
- [39] Kang, F., Wang, Q., Xiang, S., “Synthesis of mesoporous Al-MCM-41 materials using metakaolin as aluminium source”, *Material. Letters*, 59: 1426-1429, (2005).
- [40] Tapaswi, P.K., Moorthy, M.S., Park S.S., Ha, C.S., “Fast, selective adsorption of Cu²⁺ from aqueous mixed metal ions solution using 1,4,7-triazacylononane modified SBA-15 silica adsorbent (SBA-TACN)”, *J. Solid State Chem.*, 211: 191–199, (2014).
- [41] Luo, G., Yan, S., Qiao, M., Fan, K., “Ru/Sn-SBA-15 catalysts: preparation, characterization, and catalytic performance in ethyl lactate hydrogenation”, *Applied Catalysis A: General*, 332: 79–88, (2007).
- [42] Shah, P., Ramaswamy, A.V., Lazar, K., Ramaswamy, V., “Direct hydrothermal synthesis of mesoporous sn-sba-15 materials under weak acidic conditions”, *Microporous and Mesoporous Mat.*, 100: 210–226, (2007).
- [43] Ojeda, M., Campero A., Guadalupe L.J., Ortega-Alfaro, M.C., Celso, V., Alvarez, C., “Incorporation of a tungsten Fischer-type metal carbene covalently bound to functionalized SBA-15”, *Microporous and Mesoporous Mat.*, 111: 178–187, (2008).
- [44] El-Hendawy, A.A., “Influence of HNO₃ oxidation on the structure and adsorptive properties of corncob-based activated carbon”, *Carbon*, 41: 713–722, (2003).
- [45] Celis, J., Amadeo, N.E., Cukierman, A.L., “In situ modification of activated carbons developed from a native invasive wood on removal of trace toxic metals from wastewater”, *J. Hazard. Mater.*, 161: 217–223, (2009).
- [46] Başoğlu F.T., Balcı S., “Surface Properties of metal-incorporated Al-pillared interlayered clay catalysts analyzed by chemisorption and infrared analysis”, *G.U. J. Sci.*, 22(3): 215-225, (2009).
- [47] Noreña-Franco, L., Hernandez-Perez, I., Aguilera-Pliego, J., Maubert-Franco, A., “Selective hydroxylation of phenol employing Cu-MCM-41 catalysts”, *Catal. Today*, 75: 189-195, (2002).
- [48] Parry, E.P., “An infrared study of pyridine adsorbed on acidic solids. Characterization of surface acidity”, *J. Catalysis*, 2: 371-379, (1963).
- [49] Auer, H., Hofmann, H., “Pillared clays characterization of acidity and catalytic properties and comparison with some zeolites”, *Appl. Catal. A-Gen.*, 97 (1); 23–38, (1993).
- [50] Barzetti T, Selli E, Moscotti D, Forni L., “Pyridine and ammonia as probes for FTIR analysis of solid acid catalysts” *J. Chem. Soc., Faraday T.*, 92(8): 1401-1407, (1996).
- [51] Chakraborty, B., Viswanathan B., “Surface acidity of MCM-41 by in situ IR studies of pyridine adsorption”, *Catal. Today*, 49: 253-260, (1999).

- [52] Zaki, M. I., Hasan, M.A., Al-Sagheer, F.A., Pasupulety, Lata., “In situ FTIR spectra of pyridine adsorbed on SiO₂-Al₂O₃, TiO₂, ZrO₂ and CeO₂: general considerations for the identification of acid sites on surfaces of finely divided metal oxides”, *Colloids Surf. A Physicochem. Eng. Asp.*, 190: 261–274, (2001).
- [53] Gokce Y., Aktas Z., “Nitric acid modification of activated carbon produced from waste tea and adsorption of methylene blue and phenol”, *App. Sur. Sci.*, 313: 352–359, (2014).